Underground storage of hydrogen and hydrogen/methane mixtures: Influence of reservoir factors and engineering choices on feasibility, storage operations, and risks

Thomas A. Buscheck
Lawrence Livermore National Laboratory
FECM SHASTA Project
June 6, 2023

DOE Hydrogen Program
2023 Annual Merit Review and Peer Evaluation Meeting

Project FE013

LLNL-POST-849006
This work was supported by the U.S. Department of Energy, Office of Fossil Energy and Carbon Management (FECM) through the Subsurface Hydrogen Assessment, Storage, and Technology Acceleration (SHASTA) project. This work was performed under the auspices of the U.S. Department of Energy by Lawrence Livermore National Laboratory under contract DE-AC52-07NA27344. Lawrence Livermore National Security, LLC.

Overview

- Underground natural gas (NG) storage (UGS) has provided long-duration energy storage for more than 100 years, primarily to meet seasonally-variable heating demand.
- Underground hydrogen (H_2) storage (UHS) of H_2/NG mixtures can be developed using similar storage facilities and reservoir-engineering practices.
- The key thermophysical properties of NG and H_2/NG mixtures that govern differences in delivery performance between UGS and UHS are: (1) mass density, (2) viscosity, (3) interfacial tension (IFT), and lower heating value (LHV).
- These thermophysical properties affect the key metrics that quantify delivery performance, such as energy-storage density and sweep efficiency.
- A goal of this study is to quantity these properties for NG and H_2/NG mixtures and to understand their influence on delivery performance, engineering choices, and storage operations for UGS and UHS.

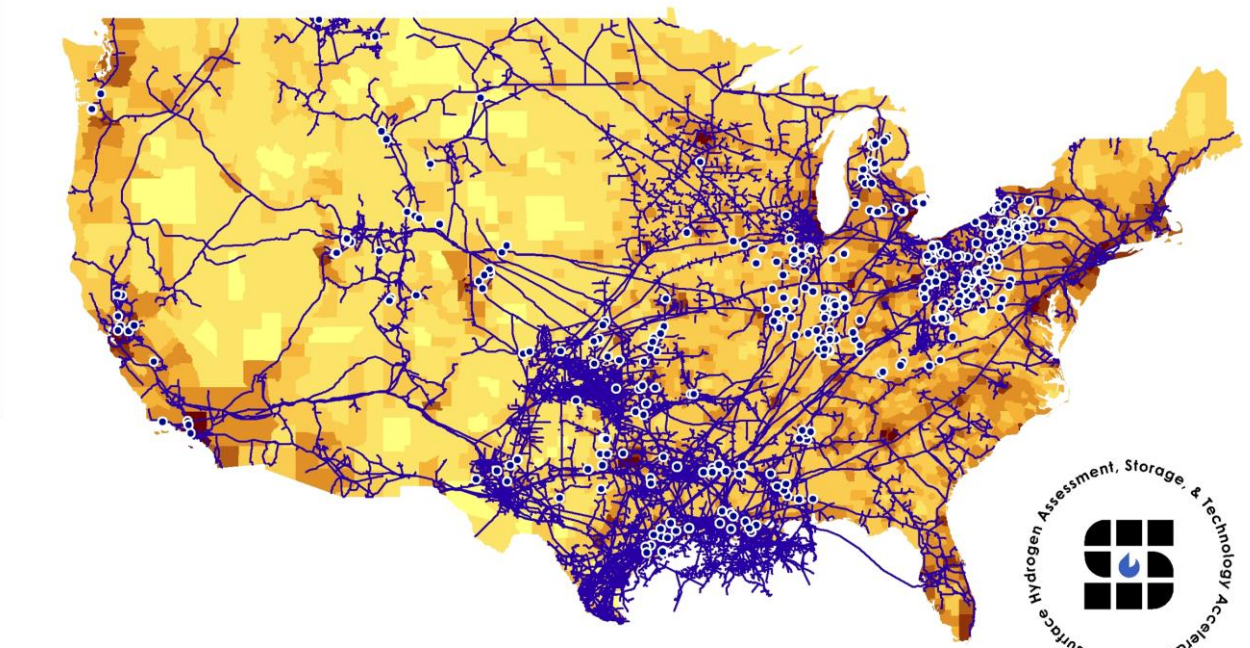

Project goal

- The goal of this project is to identify the metrics that quantify the delivery performance of NG, H_2, and N_2/NG mixtures.
- These metrics include energy-storage density and sweep efficiency, which is primary influenced by viscous fingering (quantified by the capillary number) and gravity override, which depend on reservoir depth (pressure) and temperature.
- Using these metrics, we scale the delivery performance of H_2 and H_2/NG mixtures to the delivery performance of NG in existing UGS facilities.
- The scaled reservoir-performance metrics strongly depend on the H_2 fraction in H_2/NG mixtures.
- The scaled reservoir-performance metrics can become a useful tool in future studies to
  - ✓ Screen and rank potential UHS sites.
  - ✓ Develop recommended practices for UHS.

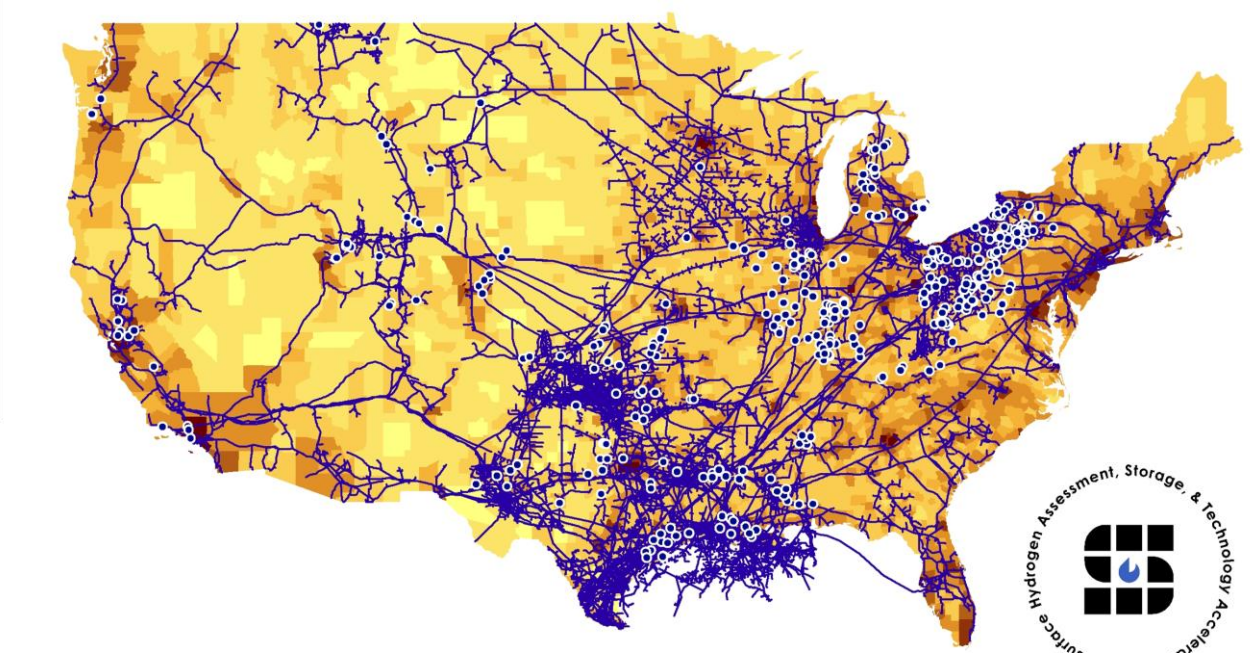

Advantages of underground gas storage, compared to tank storage

- **Storage capacity:** Porous formations (depleted hydrocarbon reservoirs and saline aquifers) can accommodate long-duration (seasonal) storage, while salt caverns can accommodate storage for up to a month.
- **Storage cost:** The geologic structure is the containment vessel.
  - ✓ Gas can be stored at greater pressure and mass density than in storage tanks.
  - ✓ Construction costs are primarily those associated with the injection/withdrawal well infrastructure, which are less than the cost of storage tanks.
- **Surface footprint:** The land area occupied by well pads and pipelines is smaller than that of storage tanks.
- **Storage safety:** The storage formation is physically separated from risk factors, such as oxygen, ignition sources, and floods, which reduces the vulnerability to fire, extreme climate events, and sabotage.



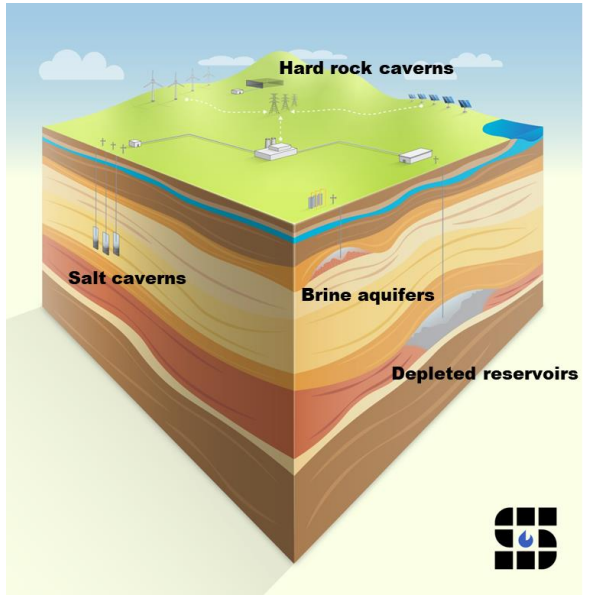

Storage-reservoir types

- Porous formations (saline aquifers and depleted hydrocarbon reservoirs) enable long-duration (seasonal) storage, while salt caverns require less cushion gas.

Table 1. Summary of cushion gas percentages, injection period, and withdrawal period for the three UGS storage types based on data from CEDIGAZ (2017) and Amid et al (2016).

Storage type	Cushion gas percentage of total gas stored	Injection period (days)	Withdrawal period (days)
Saline aquifers	50–80%	200–250	100–150
Depleted hydrocarbon reservoirs	50–70%	200–250	100–150
Salt caverns	20–30%	20–40	20–40

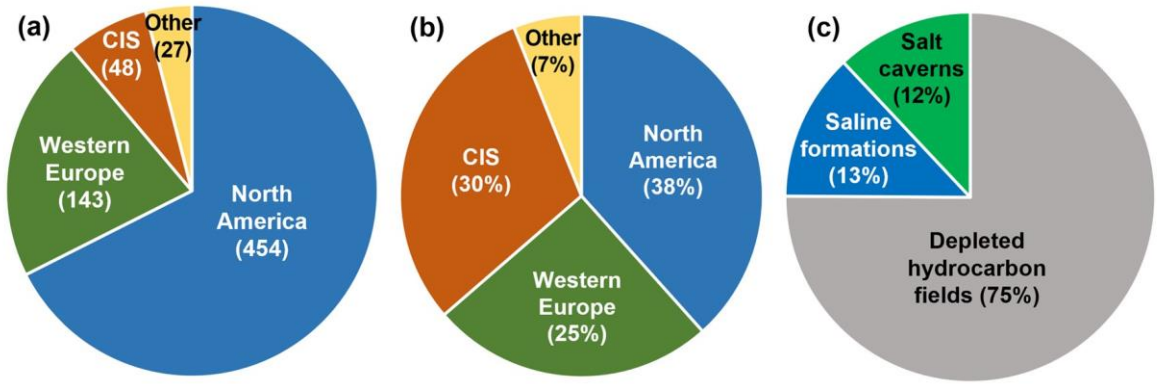

Figure 2. Summary of 672 UGS facilities operating worldwide in 2016, broken down by (a) number of facilities, (b) working-gas capacity by region, and (c) percentage of working-gas capacity by storage-reservoir type, based on data from CEDIGAZ (2017) and Amid and others (2016). CIS stands for the Commonwealth of Independent States.

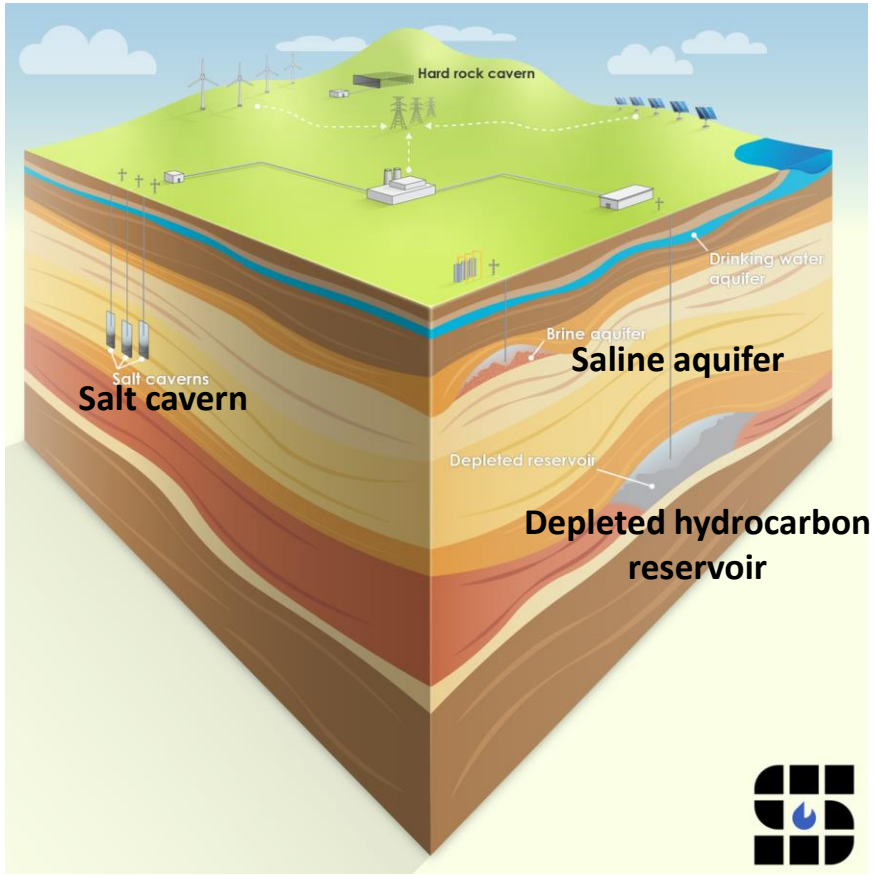

Figure 1. Three primary storage-reservoir types: saline aquifers, depleted hydrocarbon reservoirs, and salt caverns.

Porous formations are preferred for large-scale, long-duration storage

- An impermeable caprock and containment geometry (e.g., anticlinal structure) are required to contain by buoyant NG, which is primarily CH_4, as well as H_2, and NG/H_2 mixtures.
- Depleted hydrocarbon reservoirs are preferred over saline aquifers because of their proven ability to contain buoyant fluids.
- The ***spill point*** determines the maximum bulk-rock storage volume ($BRSV_{max}$).

Depleted hydrocarbon reservoir

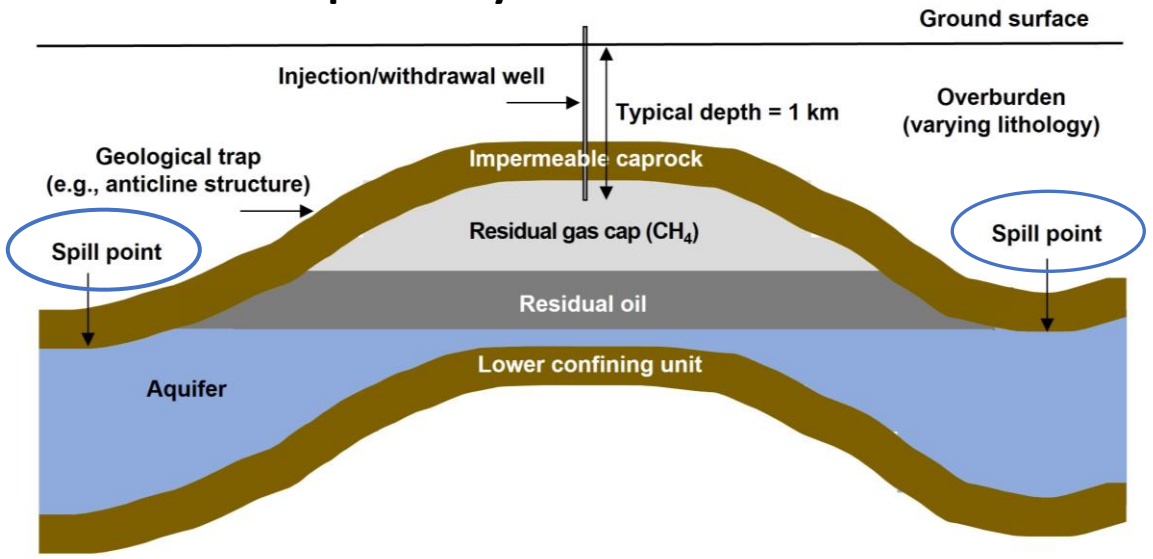

Saline aquifer storage

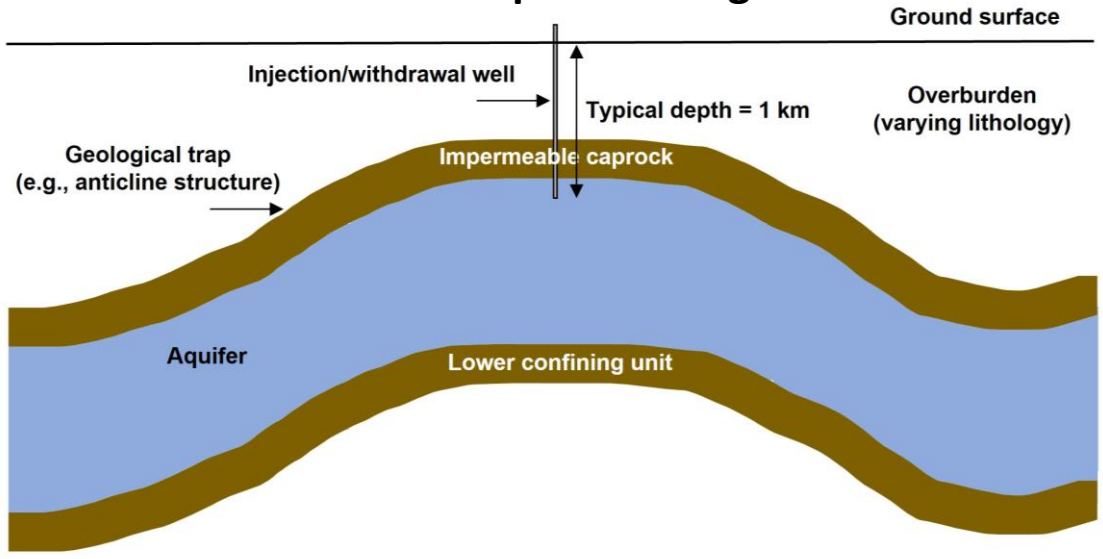

LLNL-POST-849006

UGS and UHS involve the same injection/withdrawal operations

- UGS of NG and UHS of H_2 and NG/H_2 mixtures involve the same storage geometry of working gas overlying cushion gas.
- Injection/withdrawal wells are usually near the top of the containment geometry.
- For UHS, various options for cushion-gas composition are being considered.

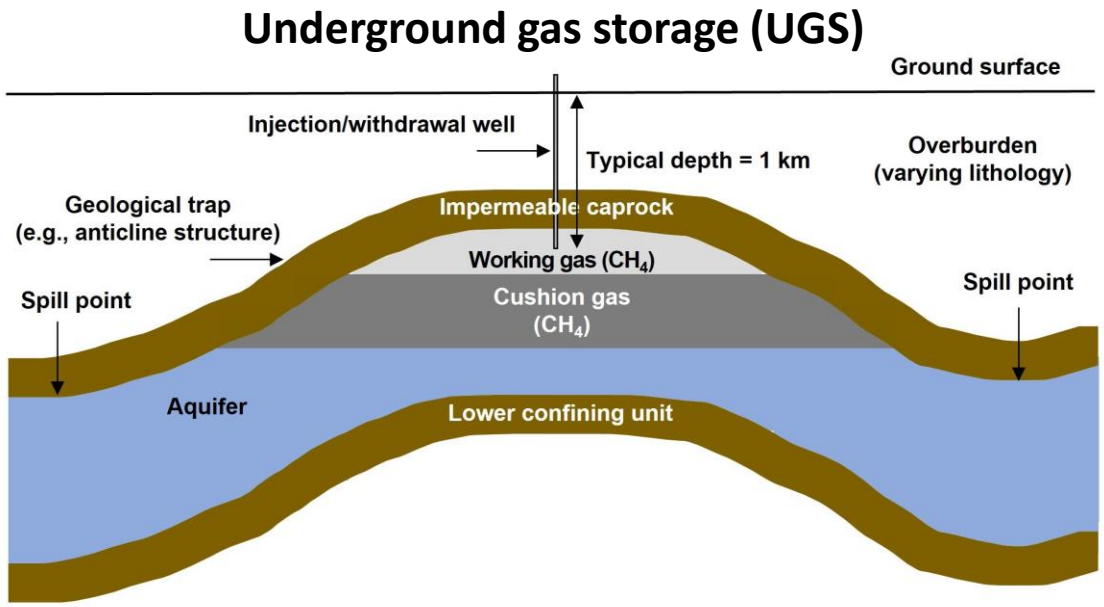

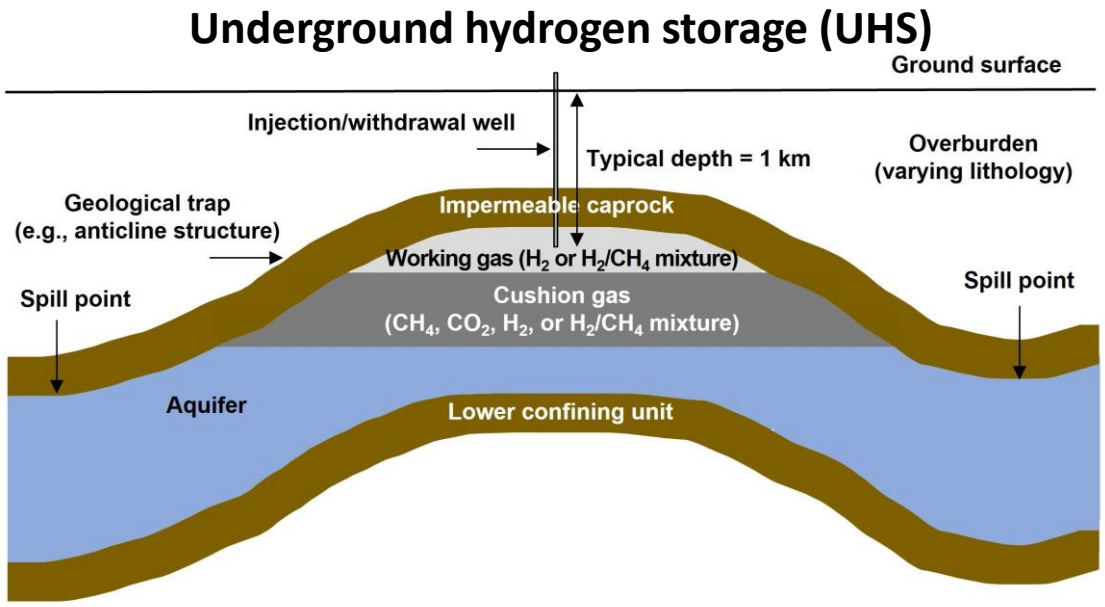

LLNL-POST-849006

Recoverable working-gas, energy-storage density

- Recoverable H_2 and CH_4 energy content per volume of rock (E_{H2} and E_{CH4}) (MJ/m^3) are given by

$$E_{H_2} = S_{eff}\rho_{H_2}\left(LHV_{H_2}\right)Y_{H_2}\varphi(1 - S_{wi})$$

$$E_{CH_4} = S_{eff}\rho_{CH_4}\left(LHV_{CH_4}\right)Y_{CH_4}\varphi(1 - S_{wi})$$

Term	Unit	Definition
$BRSV_{max}$	m^3	Maximum bulk-rock storage volume
E_{H_2}	MJ/m^3	H_2 energy content per volume of rock
ρ_{H_2}	kg/m^3	Mass density of H_2 at reservoir temperature and pressure
ρ_{CH_4}	kg/m^3	Mass density of CH_4 at reservoir temperature and pressure
LHV_{H_2}	MJ/kg	Lower heating value of H_2 (120 MJ/kg)
LHV_{CH_4}	MJ/kg	Lower heating value of CH_4 (50 MJ/kg)
Y_{H_2}	fraction	Volume fraction of H_2 in the gas phase for the working gas
Y_{CH_4}	fraction	Volume fraction of CH_4 in the gas phase for the working gas
φ	fraction	Porosity
S_{wi}	fraction	Irreducible water saturation, which depends on the wettability of the storage formation.
S_{eff}	fraction	Sweep efficiency, affected by viscous fingering and gravity override.

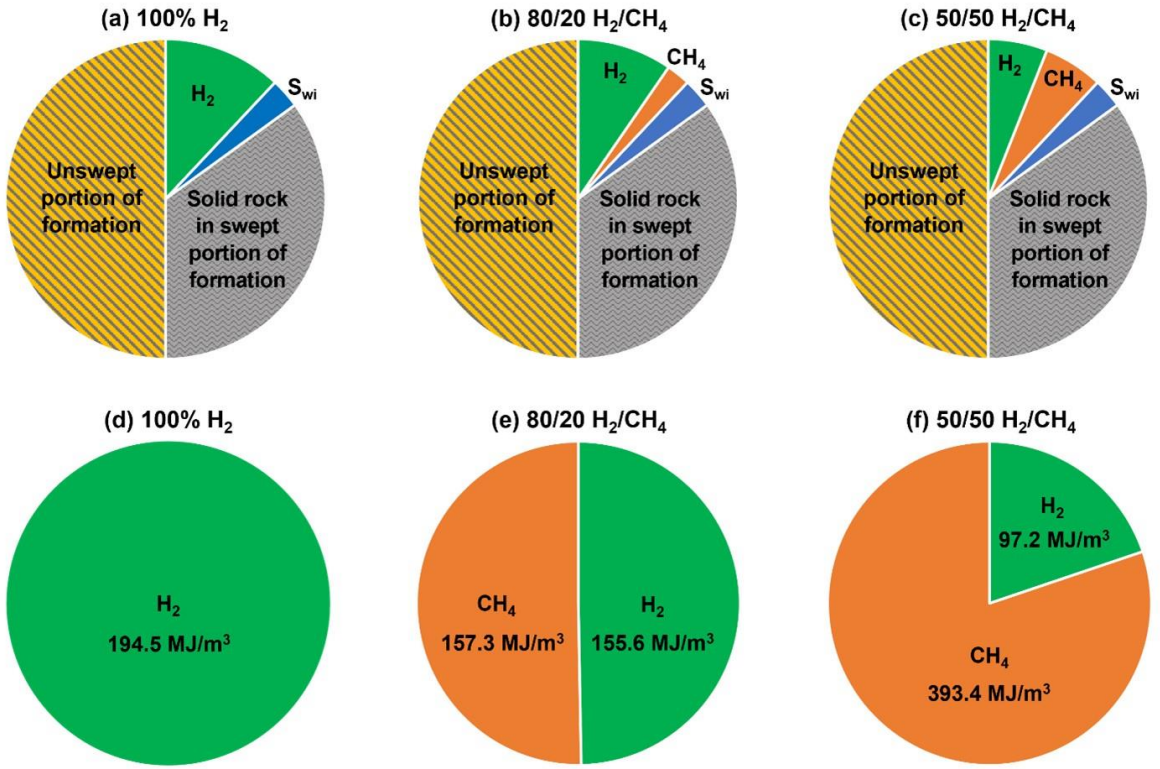

Figure 1. Proportions of the bulk-rock volume in the working-gas storge zone are shown for (a) 100% H_2, (b) an 80/20 H_2/CH_4 mix by volume, and (c) a 50/50 H_2/CH_4 mix by volume. Volumetric energy density, based on bulk-rock volume in the working-gas zone is shown for (d) 100% H_2, (b) an 80/20 H_2/CH_4 mix by volume, and (c) a 50/50 H_2/CH_4 mix by volume.

Volumetric energy density of H_2 is much less than for CH_4

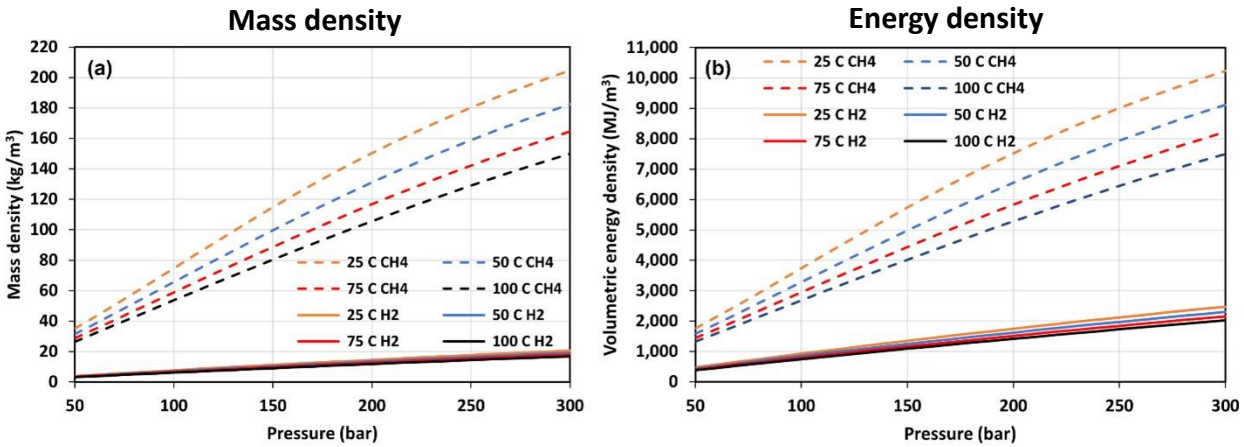

Figure 1. Mass density [ρ_{H_2} and ρ_{CH_4}] (a) and volumetric energy density of H_2 and CH_4 (b) are plotted as a function pressure and temperature.

- **H_2/CH_4-to-CH_4 volumetric energy-density ratio depends on pressure and temperature.**

Table 1. Summary of energy content in blended H_2/CH_4 mixtures by volume.

H_2/CH_4 gas mixture	H_2/CH_4-to-CH_4 volumetric energy-density ratio	CH_4-to-H_2/CH_4 volumetric energy-density ratio	H_2 energy fraction in H_2/CH_4 gas mixture
100/0	0.24–0.28	3.69–4.31	1.0
80/20	0.39–0.43	2.40–2.59	0.48–0.53
50/50	0.62–0.64	1.57–1.62	0.19–0.22
20/80	0.85–0.86	1.17–1.18	0.05–0.07

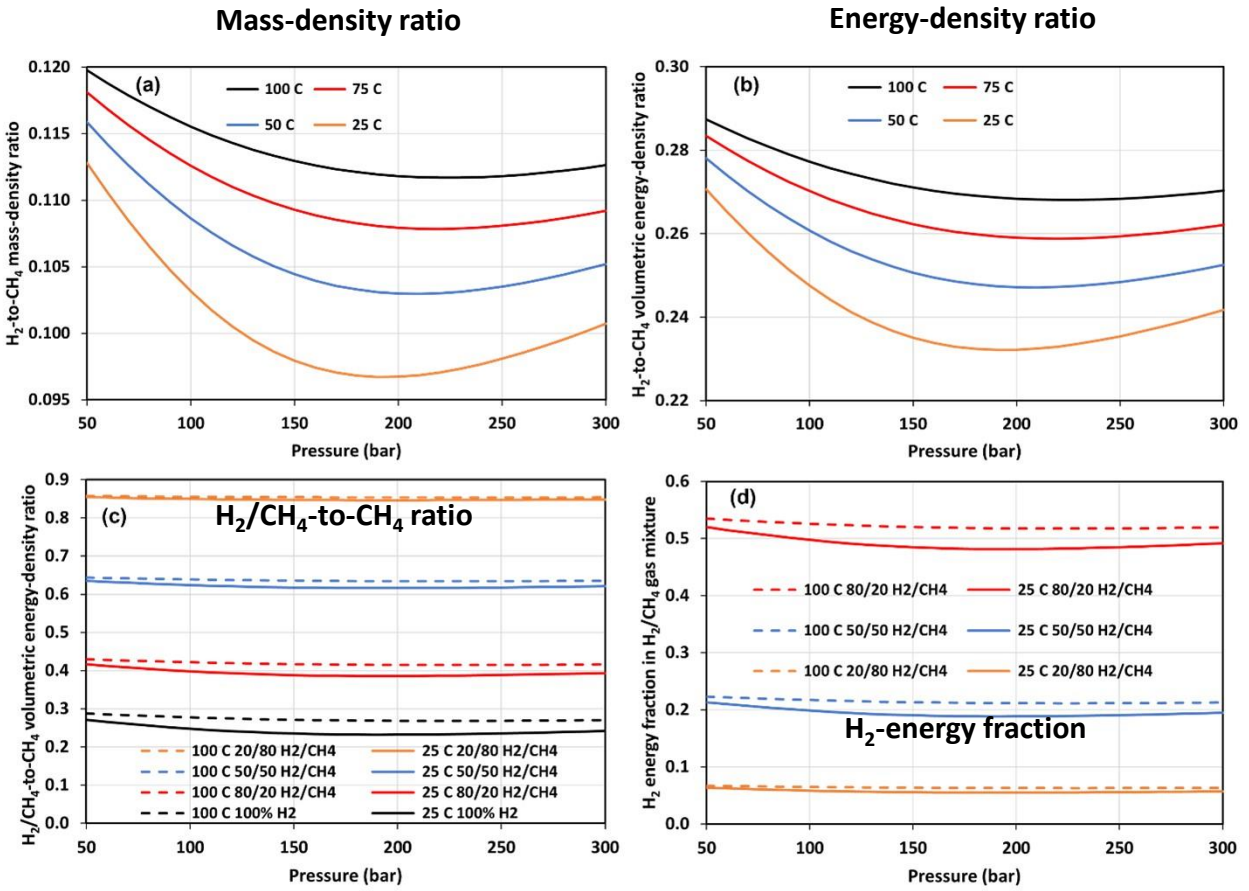

Figure 2. The H_2-to-CH_4 mass-density ratio (a) and H_2-to-CH_4 volumetric energy-density ratio (b) are plotted as a function of pressure and temperature. The H_2/CH_4-to-CH_4 volumetric, energy-density ratio (c) and the H_2 energy fraction in the H_2/CH_4 gas mixture (d) are plotted for different H_2/CH_4 mixtures by volume, as a function of pressure for temperatures of 25 and 100°C.

Gravity override of NG and H_2 decreases with storage depth

- Sweep efficiency depends on the magnitude of gravity override, viscous fingering and trapping (stranding) of NG and H_2 working gas.
- Gravity override, driven by buoyancy, depends on the mass-density ratio between water and gas.
- Mass density of CH_4 and H_2 increases linearly with storage depth (pressure), while mass density of water (formation brine) only increases by a few percent.
- Mass density of water, CH_4 and H_2 decreases weakly with increasing temperature.
- Gravity override of CH_4 (NG) and H_2 working gas decreases nearly linearly with storage depth (pressure).
- Because of the importance of gravity override, sweep efficiency will improve with storage depth (pressure).

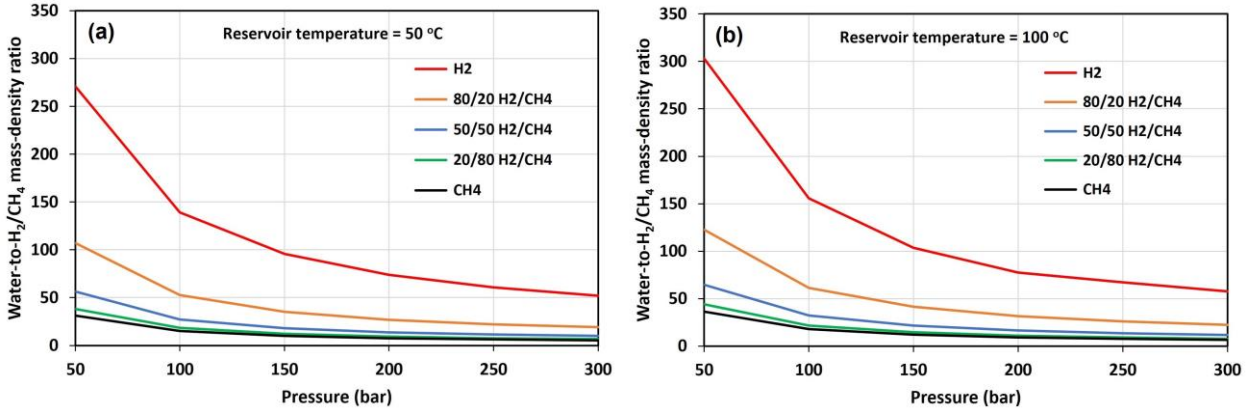

Figure 1. The water-to-H_2/CH_4 mass-density ratio for various H_2/CH_4 gas mixtures by volume is plotted as a function of pressure for reservoir temperatures of (a) 50°C and (b) 100°C.

Viscous fingering of gas in formation brine

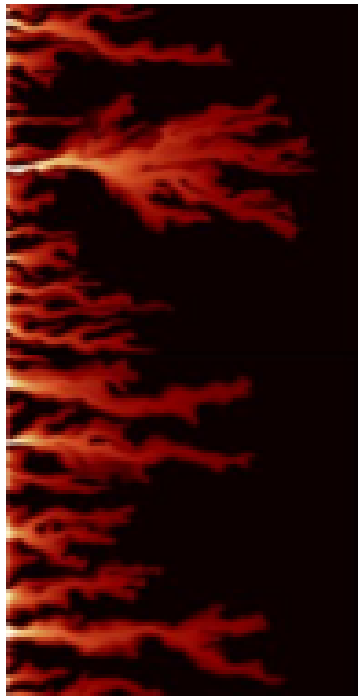

(Salmo et al. 2022)

- There is a large contrast in the viscosity of water (brine) and the displacing fluid (gas).
- The large gas-to-water mobility ratio contributes to viscous fingering of gas.
- Because the viscosity of H_2 is less than that of CH_4, it results in greater viscous fingering than CH_4.
- For both CH_4 and H_2, viscous fingering will be greater at shallow depths where temperature and pressure are less than for deep storage depths.
- For both CH_4 and H_2, sweep efficiency increases significantly with storage depth because both viscous fingering and gravity override decrease with depth.

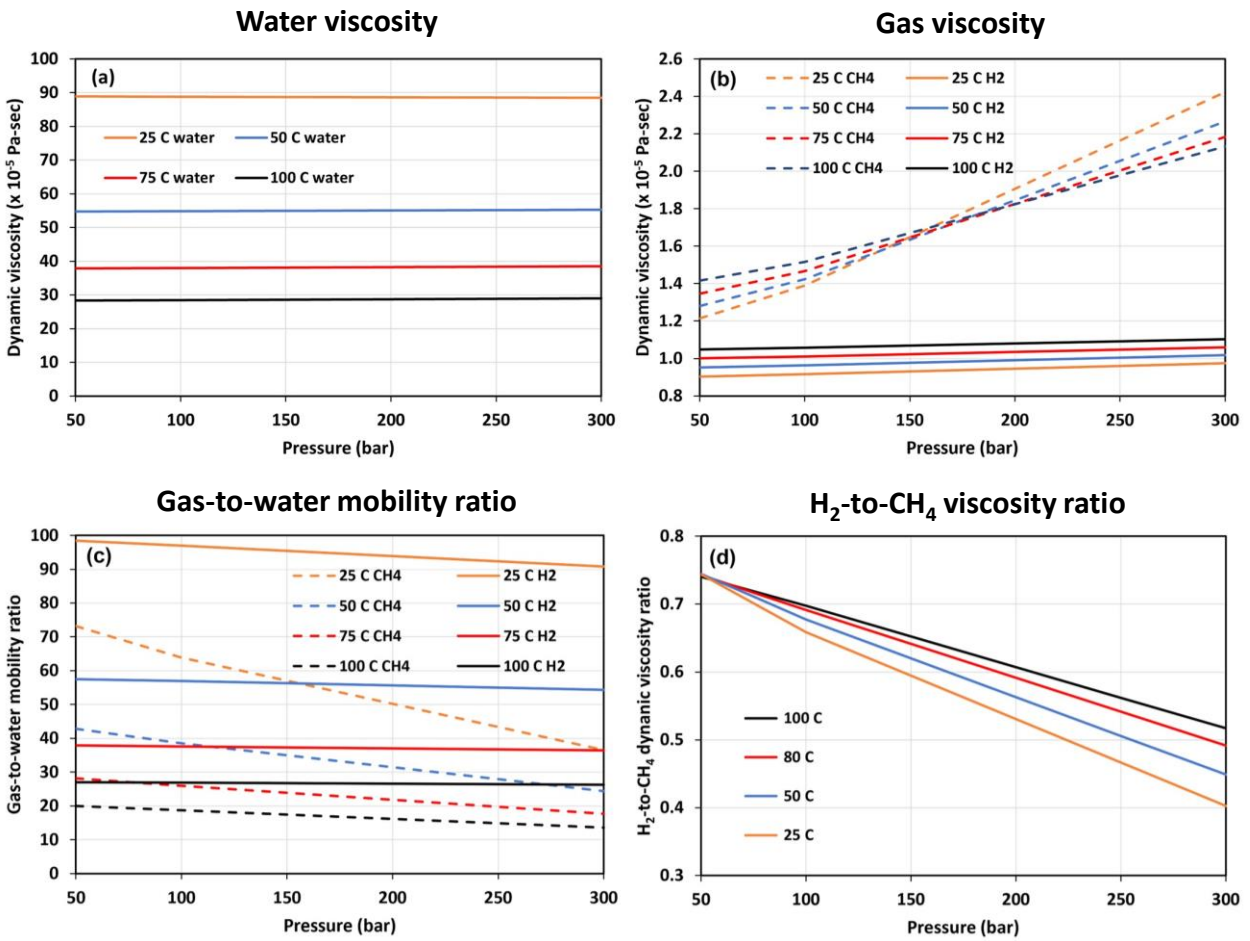

Figure 1. The dynamic viscosity of water (a), dynamic viscosity of H_2 and CH_4 (b), gas-to-water mobility ratio for H_2 and CH_4 (c), and H_2-to-CH_4 viscosity ratio (d) are plotted as a function of pressure and temperature

Viscous fingering of gas in formation brine

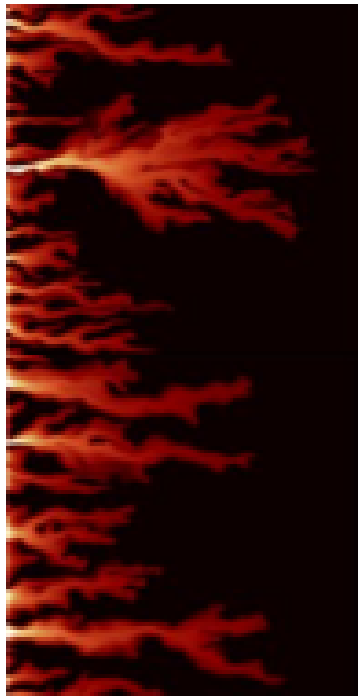

(Salmo et al. 2022)

A dimensionless group, called the capillary number, *Nc*, is used in the analysis of fluid flow to characterize the ratio of viscous force to interfacial tension force (Rezk et al. 2019; Zivar and Pourafshary, 2019; Muhammed et al. 2022) as follows:

$$N_c = V * {}^{\mu}/_{IFT}$$

where V is the Darcy velocity, μ is the dynamic viscosity of the displacing fluid (gas), and IFT is the gas-to-water interfacial tension.

- **The CH_4-to-H_2 viscosity/IFT ratio is a measure of the magnitude of viscous fingering for H_2, compared with CH_4.**

Table 1. Range of gas-to-water IFT for H_2 and CH_4. Also included are the calculated gas-to-water H_2-to-CH_4 IFT ratio and H_2-to-CH_4 viscosity to IFT ratio over the indicated range of pressure and temperatures (Chow et al. 2018).

	0 to 250 bar, 25 to 80 °C			
	IFT (mN/m)	H_2-to-CH_4 IFT ratio	H_2-to-CH_4 viscosity/IFT ratio	CH_4-to-H_2 viscosity/IFT ratio
H_2	49.4–71.3	1.04–1.88	0.27–0.53	1.9–3.7
CH_4	25.8–66.1			

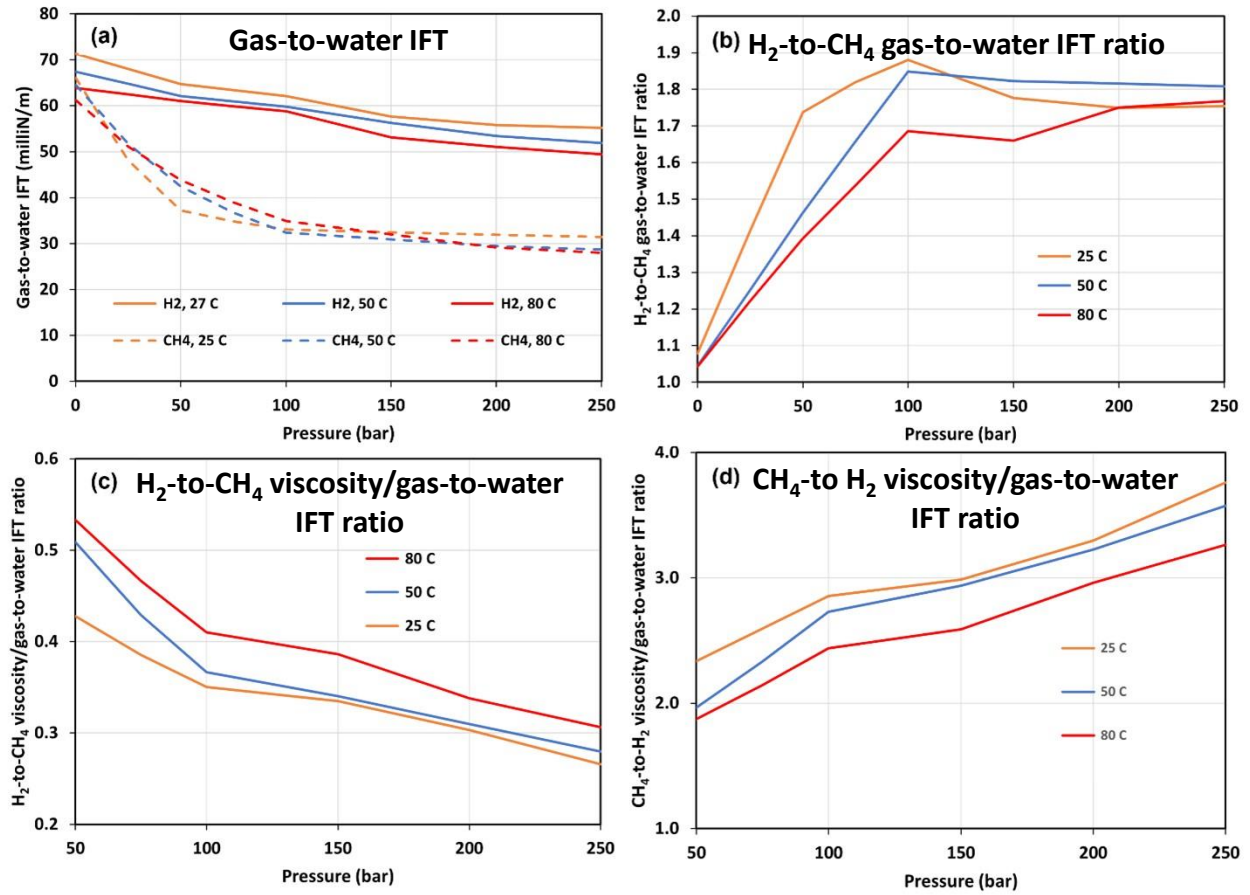

Figure 2. (a) Gas-to-water interfacial tension (IFT) for H_2 and CH_4, (b) H_2-to-CH_4, gas-to-water IFT ratio, (c) H_2-to-CH_4, gas-to-water viscosity/IFT ratio, and (d) CH_4-to-H_2, gas-to-water IFT ratio are plotted as a function of pressure from 0 to 250 bar and for temperatures of 25°C (or 27 °C), 50°C, and 80°C. Note that the lack of smoothness in the trends is the result of the limited number of pressure values for which the IFT measurements were made by Chow et al. (2018).

Capillary hysteresis contributes to the stranding of working gas

- **Drainage process:** During the injection cycle, the non-wetting phase (H_2/CH_4) displaces the wetting phase (brine), reducing the wetting-phase saturation.
- **Imbibition process:** During the withdrawal cycle, some of the pore space that had been occupied by the non-wetting phase (H_2/CH_4) is displaced by the wetting phase (brine), increasing the wetting-phase saturation.
- Capillary-pressure hysteresis (Figure 1a) and relative-permeability hysteresis (Figure 1b) occur because it takes less pressure for the wetting phase to displace the non-wetting phase during the imbibition process.
- The imbibition process collapses some of the channels of the storage formation that had been filled with H_2/CH_4 working gas, which reduces the number of pathways between the stored H_2/CH_4 working gas and the withdrawal wells, which traps (strands) pockets of working gas.
- This may lead to increased production of cushion gas and formation brine, which may reduce the deliverability of the H_2/CH_4 working gas.

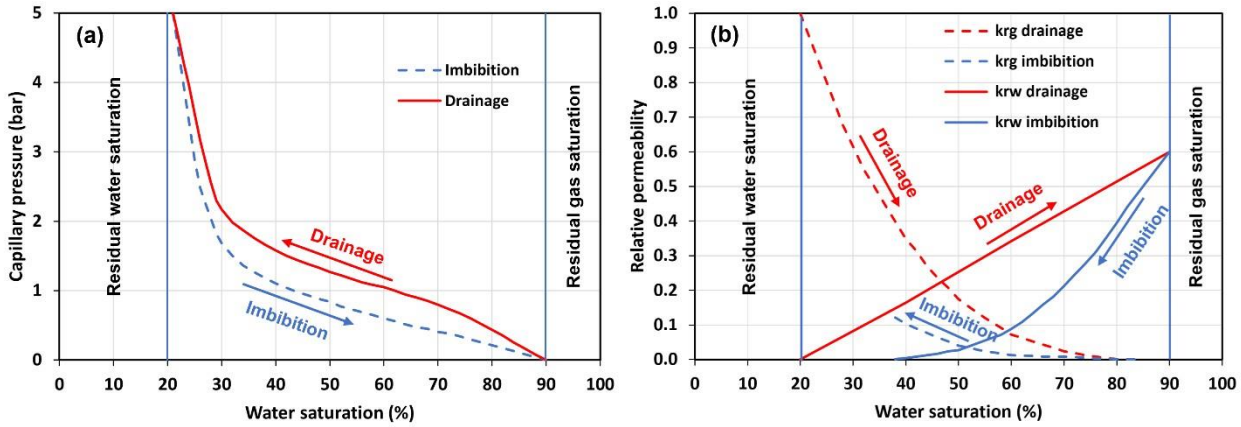

Figure 1. Hysteretic capillary-pressure curves (a) for gas-water systems, based on Figure 6 from Zivar and others (2021). Hysteretic relative-permeability curves (b) for water-gas systems, based on Figure 1a from Fatemi and Sohrabi (2018).

The volumetric H_2 fraction is a key reservoir-engineering design variable

- Total volumetric energy density depends on volumetric H_2 fraction and temperature.
- Total volumetric energy density increases linearly with pressure (depth).
- The magnitude of gravity override (due to buoyancy) increases strongly with H_2 fraction.

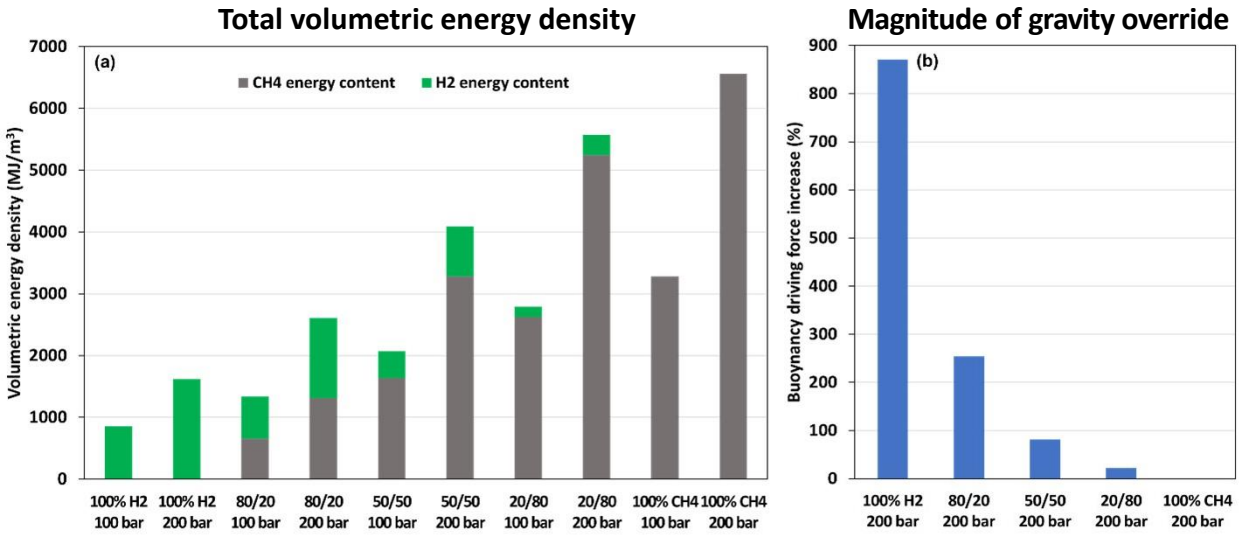

Figure 2. (a) Volumetric energy density of H_2/CH_4 mixtures for pressures of 100 and 200 bar and a temperature of 50°C and (b) buoyancy driving force increase compared to 100% CH_4 for 200 bar and 50°C. The increase in buoyancy driving force is similar for 100 and 200 bar.

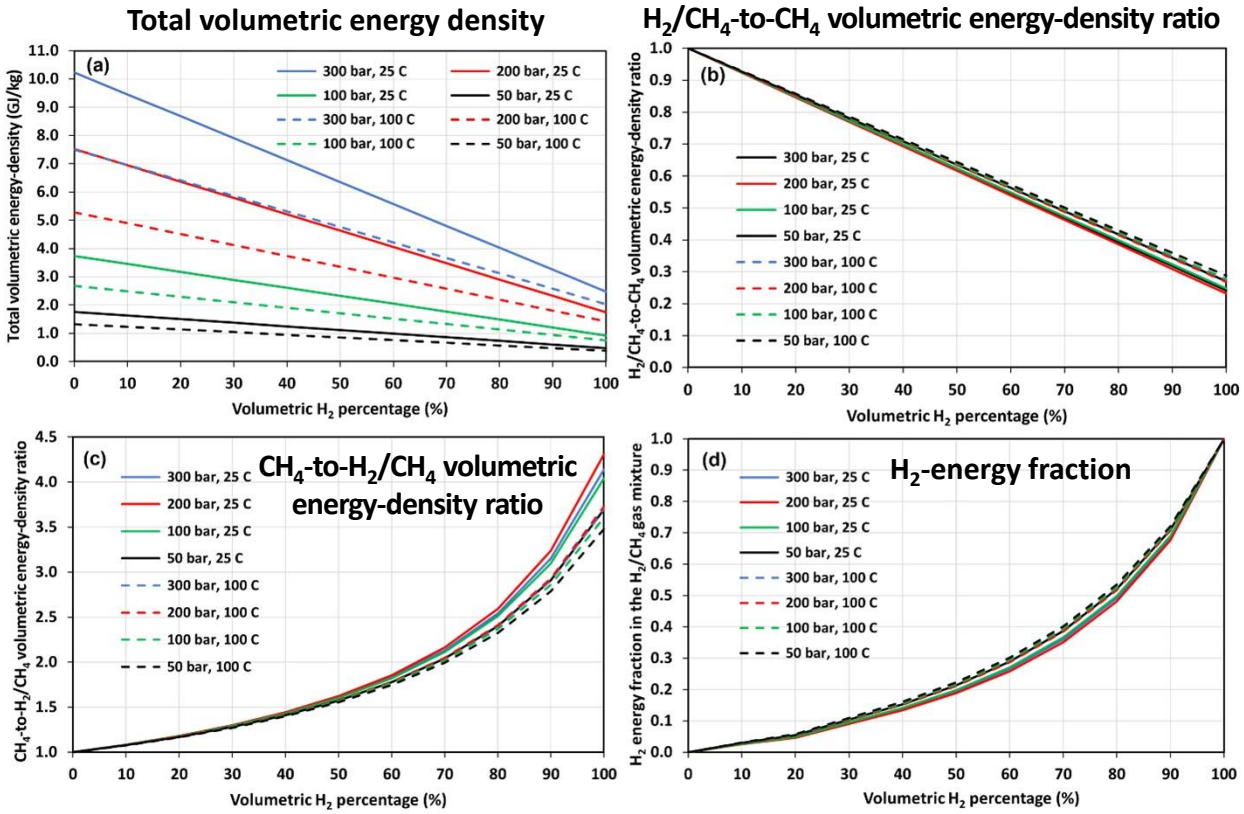

Figure 1. (a) Total volumetric energy density, (b) H_2/CH_4-to-CH_4 volumetric, energy-density ratio, (c) CH_4-to-H_2/CH_4 volumetric, energy-density ratio, and (d) H_2 energy fraction in the H_2/CH_4 gas mixture are plotted as a function of volumetric H_2 percentage for pressures from 50 to 300 bar and temperatures of 25 and 100°C. A temperature of 25°C is typical for wellbore conditions, while 100°C is representative of some reservoir conditions.

Summary and Conclusions

- Underground hydrogen storage (UHS) of H_2/NG mixtures can be developed using similar storage facilities and reservoir-engineering practices of underground gas storage (UGS).
- Key differences in delivery performance between UGS and UHS that need to be considered in making engineering choices are those affected by
  - ✓ Energy-storage density.
  - ✓ Sweep efficiency, influenced by viscous fingering, as well as gravity override.
  - ✓ Trapping of working gas, influenced by capillary-pressure and relative-permeability hysteresis.
- Key observations about the metrics that quantify delivery performance are:
  - ✓ Energy-storage density increases with storage depth for NG and H_2/NG mixtures.
  - ✓ Sweep efficiency is greater when viscous fingering and gravity override are controlled.
  - ✓ Viscous fingering and gravity override of H_2/NG mixtures increase with H_2 fraction.
  - ✓ Viscous fingering and gravity override for NG and H_2/NG mixtures decrease with storage depth.
  - ✓ Sweep efficiency and energy-storage density for NG and H_2/NG mixtures increase with storage depth.
- The reservoir-performance metrics for H_2/NG mixtures that we have developed and scaled to those of NG in existing UGS facilities can be useful in screening and ranking potential UHS sites and in developing recommended practices for UHS.

Future work and references

Future work

- Develop the relationships for scaling the delivery performance for H_2 and H_2/NG mixtures in UHS facilities to the performance of NG in UGS facilities.
- Catalog reservoir data for porous, gas-storage reservoirs: (1) UGS reservoirs, (2) depleted hydrocarbon reservoirs, and (3) saline aquifers.
- Catalog scaled delivery-performance metrics for porous gas-storage reservoirs, as a function of volumetric H_2 fraction in H_2/NG mixtures.
- Using the scaled delivery-performance metrics, rank potential UHS reservoirs.
- Develop recommended practices for UHS.

References

Buscheck, T. A. et al., 2023. Underground storage of hydrogen and hydrogen/methane mixtures: Influence of reservoir factors and engineering choices on feasibility, storage operations, and risks, *International Journal of Hydrogen Energy*, in review.